Electrochimica Acta 127 (2014) 159–166

Contents lists available at ScienceDirect

Electrochimica Acta

journal homepage: www.elsevier.com/locate/electacta

Electrochemical reduction of 2-chloro-*N*-phenylacetamides at carbon and silver cathodes in dimethylformamide

Erick M. Pasciak[a], Arkajyoti Sengupta[a], Mohammad S. Mubarak[b], Krishnan Raghavachari[a], Dennis G. Peters[a,*]

[a] Department of Chemistry, Indiana University, Bloomington, IN 47405, USA
[b] Department of Chemistry, The University of Jordan, Amman 11942, Jordan

ARTICLE INFO

Article history:
Received 7 November 2013
Received in revised form 24 January 2014
Accepted 24 January 2014
Available online 10 February 2014

Keywords:
2-Chloro-N-phenylacetamides
Carbon cathodes
Silver cathodes
Carbon–chlorine bond cleavage
Density functional theory

ABSTRACT

Cyclic voltammetry and controlled-potential (bulk) electrolysis have been employed to investigate the direct electrochemical reduction of 2-chloro-*N*-methyl-*N*-phenylacetamide (1a), 2-chloro-*N*-ethyl-*N*-phenylacetamide (1b), and 2-chloro-*N*-phenylacetamide (1c) at carbon and silver cathodes, as well as the catalytic reduction of these compounds by electrogenerated nickel(I) salen, in dimethylformamide (DMF) containing 0.050 M tetramethylammonium tetrafluoroborate ($TMABF_4$). Cyclic voltammograms for reduction of 1a and 1b show a single irreversible cathodic peak for cleavage of the carbon–chlorine bond, but two irreversible cathodic peaks are observed in cyclic voltammograms for reduction of 1c. Controlled-potential reduction of 1a and 1b gives mixtures of dechlorinated amide and *N*-alkyl-*N*-phenylaniline, whereas bulk electrolyses of 1c afford *N*-phenylacetamide in almost quantitative yield. In addition, bulk electrolyses of 1a and 1b result in the formation of very small amounts of dimeric species that arise from coupling of the radical intermediate formed by one-electron cleavage of the carbon–chlorine bond. On the basis of the coulometric *n* values and product distributions, together with computations based on density functional theory, we propose mechanistic pictures for the reduction of 1a and 1b that involve radical intermediates, whereas reduction of 1c involves carbanion intermediates.

1. Introduction

Numerous reports [1–14] dealing with the electrochemical reduction of 2-haloacetamides have been published. These investigations have revealed a surprisingly complex set of reaction pathways that depend on the structure of the compound and on the conditions employed for the electrochemical experiments. In the simplest of situations, a 2-haloacetamide undergoes a two-electron reductive cleavage of the carbon–halogen bond at a mercury or carbon cathode to afford a carbanion that, upon protonation (perhaps by the parent compound itself), yields the dehalogenated acetamide [1,2,4,5,7–9]. Electrochemical reduction of 2-haloacetamides has been utilized for the synthesis of β-lactams [3,6,12–14] as well as for the preparation of oxazolidine-2,4-diones [10]. Furthermore, cyclic dimers (e.g., piperazine-2,5-diones) have been detected [8] as products of the reduction of 2-haloacetamides, along with species that arise from cyclocoupling of the conjugate base of the 2-haloacetamide with the solvent (dimethylformamide or dimethylacetamide) [4]. Hennessy and Buchwald [15] have studied the palladium acetate-catalyzed reaction of 2-chloroacetamides as a synthetic route to the formation of oxindoles.

Acetyl groups are often used as protecting groups for amines, such as aniline, due to the mild conditions required to attach the acetyl moiety. However, harsh hydrolysis may be needed to achieve deprotection. In attempting to use electrochemical methods for such deprotection, Kopilov and Evans [16] probed the electrochemical reduction of mono-, di-, and trihaloacetanilide at a mercury cathode in solutions of 0.10 M tetraethylammonium chloride in ethanol and 0.10 M tetraethylammonium perchlorate in acetonitrile to determine whether α-haloacetanilides would undergo C–N bond cleavage to afford aniline; however, only the dehalogenated acetanilide remained upon completion of the electrolysis.

In the present investigation, we have employed cyclic voltammetry and controlled-potential (bulk) electrolysis to examine the direct electrochemical reduction of the carbon–chlorine bond of 2-chloro-*N*-methyl-*N*-phenylacetamide (**1a**), 2-chloro-*N*-ethyl-*N*-phenylacetamide (**1b**), and 2-chloro-*N*-phenylacetamide (**1c**) at carbon and silver cathodes in dimethylformamide (DMF) containing 0.050 M tetramethylammonium tetrafluoroborate ($TMABF_4$). In addition, a study has been conducted of the catalytic reduction of

* Corresponding author. Tel.: +1 812 855 9671; fax: +1 812 855 8300.
E-mail address: peters@indiana.edu (D.G. Peters).

0013-4686/$ – see front matter © 2014 Elsevier Ltd. All rights reserved.
http://dx.doi.org/10.1016/j.electacta.2014.01.133

the carbon–chlorine bonds of **1a**–**1c** by nickel(I) salen electrogenerated at reticulated vitreous carbon electrodes.

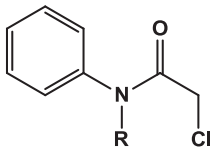

1a: R = CH_3
1b: R = C_2H_5
1c: R = H

Electrolysis products have been separated, identified, and quantitated with the aid of gas chromatography (GC) and gas chromatography–mass spectrometry (GC–MS). Surprisingly, the behavior of the methyl- and ethyl-substituted compounds (**1a** and **1b**, respectively) is not the same as that of **1c** with respect to cyclic voltammetry, coulometric *n* value, and electrolysis products. Thus, the mechanistic picture for the reduction of **1a** and **1b** appears to differ from that for the reduction of **1c**, a conclusion corroborated with the aid of calculations based on density functional theory.

2. Experimental

2.1. Reagents

Each of the following chemicals was employed, as received, without further purification: anhydrous diethyl ether (absolute, EMD Chemicals), *n*-hexadecane (99%, Sigma), chloroacetyl chloride (98%, Aldrich), chloroform-*d* (99.8%, Aldrich), acetyl chloride (98%, EMD Chemicals), succinyl chloride (95%, Aldrich), [[2,2′-[1,2-ethanediylbis(nitrilomethylidyne)]bis[phenolato]]-(*N*,*N*′*O*,*O*′)]nickel(II) (nickel(II) salen, 98%, Aldrich), potassium hydroxide (97%, Alfa Aesar), deuterium oxide (D_2O, 99.9 atom%, Aldrich), tetramethylammonium hydroxide (TMAOH, 97%, Sigma), 1,1,1,3,3,3-hexafluoro-2-propanol (HFIP, 99 + %, Alfa Aesar).

Vacuum distillation was used to purify the following compounds: aniline (99%, Alfa Aesar), *N*-methylaniline (99%, Aldrich), and *N*-ethylaniline (97%, Alfa Aesar). Dimethylformamide (DMF, 99.9%, EMD Chemicals) was utilized without further purification as the solvent for all electrochemical experiments. Tetramethylammonium tetrafluoroborate ($TMABF_4$, >99%, GFS Chemicals), which served as the supporting electrolyte, was recrystallized from water–methanol and stored in a vacuum oven at 70–80 °C prior to use. All deaeration procedures were accomplished with zero-grade argon (Air Products).

2.2. Cells, electrodes, procedures, and instrumentation

A description and photograph of the cell used for cyclic voltammetry appear in a previous publication [17]. We constructed planar, circular glassy carbon and silver cathodes (each with a geometric area of 0.071 cm^2) by press-fitting a short piece of either a glassy carbon rod (Grade GC-20, 3.0-mm-diameter, Tokai Electrode Manufacturing Company, Tokyo, Japan) or a silver rod (3.0-mm-diameter, 99.9% purity, Alfa Aesar) into the end of a machined Teflon tube. Electrical connections to these working electrodes were made via a 3.0-mm-diameter stainless-steel pole that contacted the cathode material and extended upward through the tube. A coil of platinum wire served as the auxiliary (counter) electrode for cyclic voltammetry. Prior to each scan, the glassy carbon and silver working electrodes were cleaned with an aqueous suspension of 0.05-μm alumina on a polishing pad, followed by a rinse with distilled water in an ultrasonic bath. All potentials are reported with respect to a reference electrode that consisted of a cadmium-saturated mercury amalgam [denoted as Cd(Hg) for

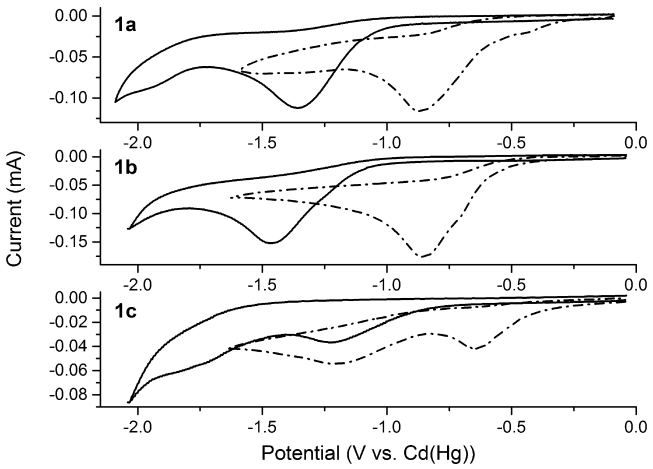

Fig. 1. Cyclic voltammograms recorded at 100 mV s^{-1} for reduction of 2.0 mM solutions of 2-chloro-*N*-methyl-*N*-phenylacetamide (**1a**), 2-chloro-*N*-ethyl-*N*-phenylacetamide (**1b**), and 2-chloro-*N*-phenylacetamide (**1c**) at a glassy carbon cathode (solid curves, scanned from ca. 0 to −2.1 to 0 V) and at a silver cathode (dash–dot curves, scanned from ca. 0 to −1.6 to 0 V) in DMF containing 0.050 M $TMABF_4$.

Figs. 1–3], in contact with DMF saturated with both cadmium chloride and sodium chloride [18–20]; this electrode has a potential of −0.76 V versus an aqueous saturated calomel electrode (SCE) at 25 °C. Cyclic voltammetric experiments were performed as described in a previous paper [21].

Information about the cell, instrumentation, and procedures used for controlled-potential (bulk) electrolysis is provided elsewhere [21,22]. We constructed carbon working cathodes by cutting disks to have approximately a 2.4-cm diameter, a 0.4-cm thickness, and a 200-cm^2 surface area from reticulated vitreous carbon logs (RVC 2X1–100S, ERG Aerospace Corporation, Oakland, CA); preparing, cleaning, and storing of these electrodes are described in a previous publication [23]. Silver gauze working electrodes (approximate surface area of 20 cm^2) were constructed from commercially available material (Alfa Aesar, 99.9%, 20 mesh woven from 0.356-mm diameter wire). For all experiments, the aforementioned cadmium-saturated mercury amalgam reference electrode

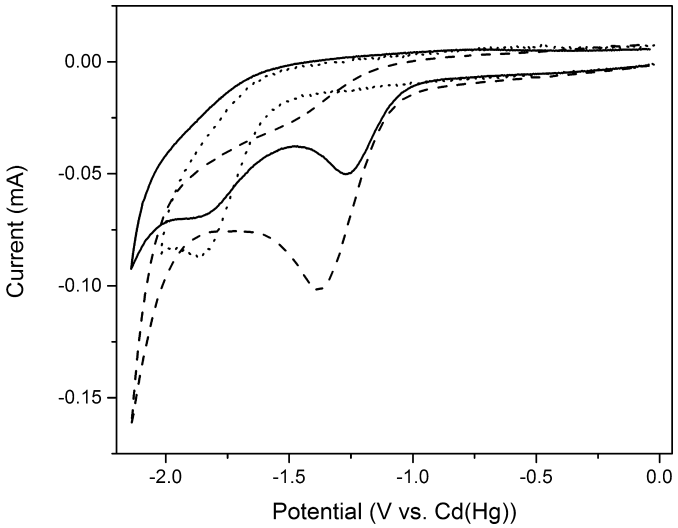

Fig. 2. Cyclic voltammograms recorded at 100 mV s^{-1} and scanned from ca. 0 to −2.0 to 0 V for reduction of 3.0 mM solutions of 2-chloro-*N*-phenylacetamide (**1c**) at a glassy carbon cathode in DMF containing 0.050 M $TMABF_4$: (A) no added HFIP or TMAOH (solid curve), (B) 30 mM HFIP added (dashed curve), (C) 10 mM TMAOH added (dotted curve).

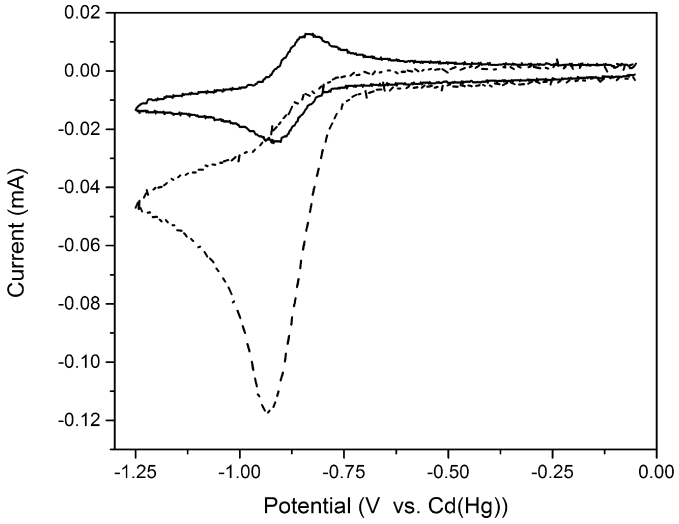

Fig. 3. Cyclic voltammograms recorded at 100 mV s^{-1} for reduction of 1.0 mM nickel(II) salen in the absence (solid curve) and in the presence of 2.0 mM 2-chloro-*N*-methyl-*N*-phenylacetamide (**1a**, dashed curve) at a glassy carbon cathode scanned from ca. −0.05 to −1.25 to −0.05 V in DMF containing 0.050 M $TMABF_4$.

was utilized, and the auxiliary anode was a graphite rod immersed in a DMF–0.050 M $TMABF_4$ solution separated from the cathode compartment by a sintered-glass disk backed by a methyl cellulose–DMF–0.050 M $TMABF_4$ plug.

2.3. Separation, identification, and quantitation of electrolysis products

At the end of each controlled-potential (bulk) electrolysis, the catholyte was partitioned three times between diethyl ether and brine. Then the ether phase was dried over anhydrous sodium sulfate and concentrated with the aid of rotary evaporation. Products were separated and identified by means of gas chromatography (GC) and gas chromatography–mass spectrometry (GC–MS). Each chromatograph (Agilent 7890A) was equipped with a 30 m × 0.25 mm capillary column (J & W Scientific) with a DB-5 stationary phase; the GC system utilized a flame-ionization detector, whereas the GC–MS system contained an inert mass-selective detector operating in electron ionization mode (70 eV). Gas chromatographic retention times and mass spectral data for the electrolysis products were compared with those for commercially available or chemically synthesized authentic samples.

Procedures used for the quantitation of electrolysis products have been described in an earlier paper [24]. Peak areas for the different products were determined with respect to an internal standard (*n*-hexadecane) added in known amount to the electrolysis cell prior to the start of a controlled-potential reduction.

Identities of the several starting materials and products, synthesized as described below, were confirmed by means of both ^1H and ^{13}C NMR spectrometry (400 MHz, Varian Inova) and high-resolution GC–MS (Thermo Electron Corporation) coupled to a MAT-95XP magnetic-sector mass spectrometer.

2.4. General procedure for synthesis of chloroacetamides (**1a**–**1c**)

We synthesized and purified 2-chloro-*N*-methyl-*N*-phenylacetamide (**1a**), 2-chloro-*N*-ethyl-*N*-phenylacetamide (**1b**), and 2-chloro-*N*-phenylacetamide (**1c**) according to the procedure outlined by Hennessy and Buchwald [15], which entails the reaction of 1 equivalent of *N*-alkylaniline or aniline with 1.5 equivalents of chloroacetyl chloride in a 2:1 ethyl acetate–water mixture and in the presence of 3 equivalents of KOH in an ice–water bath. Each reaction mixture was stirred for 1 h at 0 °C and then transferred to a separatory funnel; the organic layer was separated, washed twice with brine, dried over anhydrous sodium sulfate, and concentrated with the aid of rotary evaporation. Products **1a** and **1c** were purified by recrystallization of each resulting solid, respectively, from ethanol and water, whereas **1b** was obtained as a yellow oil via vacuum distillation. Melting points for the two solids were found to be as follows: **1a** (Mp 66–67 °C); **1c** (Mp 133–134 °C). High-resolution mass spectral data for these three compounds are as follows: (a) for **1a**, HRMS (ESI) *m/z*: calculated for $C_9H_{10}ClNO$ $[M]^+$ 183.0445, found 183.0449; (b) for **1b**, HRMS (ESI) *m/z*: calculated for $C_{10}H_{12}ClNO$ $[M]^+$ 197.0602, found 197.0597; (c) for **1c**, HRMS (ESI) *m/z*: calculated for C_8H_8ClNO $[M]^+$ 169.0289, found 169.0288.

2.5. General procedure for synthesis of products (**3a**–**3c**)

We prepared *N*-methyl-*N*-phenylacetamide (**3a**), *N*-ethyl-*N*-phenylacetamide (**3b**), and *N*-phenylacetamide (**3c**) according to the protocol described in the preceding section by substituting acetyl chloride for chloroacetyl chloride. Compounds **3a** and **3c** were obtained as colorless crystals, and **3b** was isolated as a yellow oil by means of vacuum distillation. High-resolution mass spectral data for these three compounds are as follows: (a) for **3a**, HRMS (ESI) *m/z*: calculated for $C_9H_{11}NO$ $[M]^+$ 149.0835, found 149.0834; (b) for **3b**, HRMS (ESI) *m/z*: calculated for $C_{10}H_{13}NO$ $[M]^+$ 163.0992, found 163.0991; (c) for **3c**, HRMS (ESI) *m/z*: calculated for C_8H_9NO $[M]^+$ 135.0679, found 135.0681.

2.6. Syntheses of *N,N′*-dimethyl-*N,N′*-diphenylsuccinamide (**5a**) and *N,N′*-diethyl-*N,N′*-diphenylsuccinamide (**5b**)

We prepared the title compounds according to the following general procedure based, with some modification, on that employed for the synthesis of compounds **1a**–**1c**. Freshly distilled *N*-methylaniline or *N*-ethylaniline (18.5 mmol) was added to 40 mL of cold ethyl acetate (in an ice bath). To this mixture was added sodium hydroxide (4 g, 100 mmol) dissolved in 20 mL of water, and the solution was allowed to cool to near 0 °C. Succinyl chloride (1.5 mL, 13.6 mmol) was slowly added, with stirring, to the reaction mixture and stirring was continued for 1 h. After the organic layer was separated, it was washed twice with brine, and dried over anhydrous sodium sulfate. Solvent was removed under reduced pressure, and the solid product was recrystallized from ethanol–water. A melting point and spectroscopic data were acquired for each compound: (a) for **5a**, Mp 155–156 °C; ^1H NMR ($CDCl_3$): δ 2.33 (s, 4H), 3.23 (s, 6H), 7.23–7.42 (m, 10H); ^{13}C NMR ($CDCl_3$): δ 29.5, 37.2, 127.4, 128.5, 129.7, 143.9, 172.8; HRMS (ESI) *m/z*: calculated for $C_{18}H_{20}N_2NaO_2$ $[M+Na]^+$ 319.1422; found 319.1412; (b) for **5b**, Mp 104–105 °C; ^1H NMR ($CDCl_3$): δ 1.05 (t, J = 7.2 Hz, 6H), 2.26 (s, 4H), 3.72 (q, J = 7.2 Hz, 4H), 7.19–7.42 (m, 10H); ^{13}C NMR ($CDCl_3$): δ 13.1, 29.9, 44.0, 127.8, 128.6, 129.7, 142.3, 171.4; HRMS (ESI) *m/z*: calculated for $C_{20}H_{24}N_2NaO_2$ $[M+Na]^+$ 347.1735; found 347.1728.

2.7. Computational methods

Computational studies involving density functional theory were performed to understand the mechanistic origin of the different products observed for electrochemical reduction of the three 2-chloro-*N*-phenylacetamides (**1a**–**1c**). All calculations were carried out with the Gaussian suite of electronic structure programs [25]. Geometry optimizations were done with the popular B3LYP density functional [26,27] that uses a standard 6-31 + G(d,p) basis set [28,29]. At this level of theory, the nature of the stationary points (minima or transition states) as well as zero-point vibrational

effects and thermal corrections were determined. Single-point calculations were then carried out with a larger 6-311++G(3df,2p) basis set [30,31] [triple zeta + diffuse functions (*sp* functions on C, O, and Cl, *s* functions on H) + multiple polarization functions (3*d*,1*f* on C, O, and Cl, 2*p* on H)] to obtain more reliable relative energies. Solvent effects arising from DMF ($\varepsilon = 37$) were then incorporated into these larger basis set calculations by use of the continuum solvation model with the SCRF–SMD framework as formulated by Marenich and co-workers [32]. Final Gibbs free energies of solutes in the solvent continuum are reported at the B3LYP/6-311++G(3df,2p) level by addition of thermal and entropic terms, obtained through the gas-phase calculations, to the single-point energies in the condensed-phase calculations. All transition states were characterized as possessing one and only one imaginary frequency characteristic of a true first-order saddle point. Identities of these transition states were further confirmed as representing the desired reaction coordinate by use of intrinsic reaction coordinate (IRC) analysis [33,34].

3. Results and discussion

3.1. Cyclic voltammetric behavior of 2-chloro-N-methyl-N-phenylacetamide (**1a**) and 2-chloro-N-ethyl-N-phenylacetamide (**1b**) at glassy carbon and silver cathodes

Displayed in Fig. 1 are cyclic voltammograms recorded at 100 mV s^{-1} for reduction of 2.0 mM solutions of **1a** and **1b** at either a glassy carbon electrode (solid curves) or a silver cathode (dash–dot curves) in DMF containing 0.050 M $TMABF_4$. For reductions of **1a** and **1b** at a glassy carbon electrode, a single irreversible cathodic peak is seen with a peak potential (E_{pc}) of −1.36 and −1.46 V, respectively, which we attribute to reductive cleavage of the carbon–chlorine bond. Reduction of **1a** at a silver cathode shows a definite pre-peak ($E_{pc} = -0.35$ V), followed by a main cathodic peak ($E_{pc} = -0.87$ V); although the main peak is clearly associated with reductive cleavage of the carbon–chlorine bond (as discussed later in this paper), the process associated with the pre-peak is not yet known. Reduction of **1b** at silver gives rise to two merged peaks, with the more negative peak at −0.84 V. In addition, electrochemical cleavage of the carbon–chlorine bond of **1a** and **1b** is decidedly more facile at silver than at glassy carbon, with corresponding peak potentials differing by 500–600 mV; this trend is common to the reduction of halogenated organic compounds studied in our laboratory [21,35–37] and by other groups [38–40].

3.2. Cyclic voltammetric behavior of 2-chloro-N-phenylacetamide (**1c**) at glassy carbon and silver cathodes

As depicted in Fig. 1, when cyclic voltammograms for reduction of **1c** at carbon and silver electrodes are recorded, two well separated peaks are seen; values for E_{pc} are −1.22 and −1.76 V at glassy carbon and −0.65 and −1.20 V at silver. In contrast to the behavior of **1a** and **1b**, reduction of **1c** exhibits two discrete steps at both glassy carbon and silver cathodes. As described above, electrochemical cleavage of the carbon–chlorine bond of **1c** is decidedly more facile at silver than at glassy carbon; note that both of the cathodic peaks are shifted to less negative potentials for silver cathodes.

We have examined the cyclic voltammetric behavior of **1c** in the presence of an added proton donor (HFIP) or an added base (TMAOH). Fig. 2 compares a cyclic voltammogram recorded with a glassy carbon electrode at 100 mV s^{-1} for the reduction of 3.0 mM **1c** in DMF–0.050 M $TMABF_4$ containing no added acid or base (solid curve) with those for which **1c** was reduced in the presence of 30 mM HFIP (dashed curve) or 10 mM TMAOH (dotted curve). Remarkably, only the first cathodic peak is seen when HFIP is added, whereas only the second cathodic peak is observed when TMAOH is added. As discussed more extensively later, it appears that the first cathodic peak is due to reduction of the parent compound (**1c**), whereas the second cathodic peak can be attributed to reduction of the (2-chloroacetyl)(phenyl)amide anion (**1c**$^-$, which arises from deprotonation of **1c**).

3.3. Cyclic voltammetric behavior of nickel(II) salen at glassy carbon in the presence of 2-chloro-N-phenylacetamides (**1a**–**1c**)

In a separate series of experiments, we examined the cyclic voltammetric behavior of nickel(II) salen at a glassy carbon electrode in DMF–0.050 M $TMABF_4$ to establish experimental conditions required to carry out the bulk catalytic reduction of each of the three 2-chloro-*N*-phenylacetamides (**1a**–**1c**) by electrogenerated nickel(I) salen. Shown in Fig. 3 are cyclic voltammograms recorded at 100 mV s^{-1} for the reduction of 1.0 mM nickel(II) salen at a glassy carbon electrode in DMF–0.050 M $TMABF_4$ in the absence (solid curve) and in the presence (dashed curve) of 2.0 mM 2-chloro-*N*-methyl-*N*-phenylacetamide (**1a**). We found that the electrochemical response of nickel(II) salen in the absence and presence of **1a** (as well as the other two substrates) is similar to that depicted in a recent paper [41] from our laboratory. However, in the present research, we observed no cyclic voltammetric peak for reduction of a nickel(II) salen species with an imino (C=N) bond modified by a fragment derived from a substrate molecule [42].

3.4. Controlled–potential (bulk) electrolyses of 2-chloro-N-phenylacetamides (**1a**–**1c**)

A series of controlled-potential (bulk) electrolyses of 5.0 mM solutions of the three 2-chloro-*N*-phenylacetamides at reticulated vitreous carbon and at silver gauze cathodes in DMF containing 0.050 M $TMABF_4$ was conducted. In addition, bulk electrolyses of nickel(II) salen at reticulated vitreous carbon cathodes in the presence of each of the 2-chloro-*N*-phenylacetamides were carried out. Compiled in Table 1 are coulometric data and product distributions for all of these experiments. Each entry corresponds to the average of at least two separate experiments. Product yields, which were reproducible to ±5% absolute, represent the amount of 2-chloro-*N*-phenylacetamide incorporated into each species.

Electrolyses of either **1a** or **1b** at both carbon and silver cathodes at potentials corresponding to those listed in Table 1 led to coulometric *n* values close to 1.0, whereas the nickel(I) salen-catalyzed reductions of **1a** or **1b** showed *n* values ranging from 0.9 to 1.2. On the other hand, because reduction of **1c** gives rise to two irreversible cyclic voltammetric peaks, bulk electrolyses were carried out at two different potentials for both carbon and silver electrodes; at less negative potentials, the coulometric *n* values tended to be close to 1, whereas the *n* values approached 2 for electrolyses performed at more negative potentials (including those accomplished with electrogenerated nickel(I) salen). These *n* values suggest that radical intermediates are involved in the electroreduction of **1a** and **1b**. However, because reduction of **1c** is a more intricate process, no conclusions can be reached solely on the basis of the *n* values.

Table 1 reveals that (a) direct reduction of **1a** at reticulated vitreous carbon and silver gauze cathodes or (b) nickel(I) salen-catalyzed reduction of **1a** leads to the formation of *N*-methyl-*N*-phenylacetamide (**3a**) and *N*-methylaniline (**4a**), along with a small amount (if any) of a dimeric species (**5a**). Similarly, reduction of **1b** under the same experimental conditions afforded *N*-ethyl-*N*-phenylacetamide (**3b**) as the major product, *N*-ethylaniline (**4b**) in substantial yield, and a trace of a dimer (**5b**). On the other hand, direct electroreduction of **1c** at either carbon or silver and at potentials corresponding to the first cathodic

Table 1
Coulometric *n* values and product distributions for electrochemical reduction of 5.0 mM solutions of 2-chloro-*N*-methyl-*N*-phenylacetamide (**1a**), 2-chloro-*N*-ethyl-*N*-phenylacetamide (**1b**), and 2-chloro-*N*-phenylacetamide (**1c**) at reticulated vitreous carbon and silver gauze cathodes in DMF containing 0.050 M $TMABF_4$.

				Product distribution (%)[a]				
Starting material	Cathode	*E*, V	*n*	**1**	**3**	**4**	**5**	Total
1a	C	−1.56	1.0	ND[c]	48	30	2	80
1a	Ag	−1.07	1.0	ND	61	36	ND	97
1a	C[b]	−1.13	1.2	ND	48	37	2	86
1b	C	−1.47	1.0	ND	52	21	2	75
1b	Ag	−0.87	1.1	ND	73	16	ND	89
1b	C[b]	−1.13	0.9	ND	28	40	1	69
1c	C	−1.46	1.2	30	78	ND	ND	108
1c	C	−1.84	1.8	ND	107	ND	ND	107
1c	Ag	−0.74	1.1	32	51	ND	ND	83
1c	Ag	−1.30	1.5	5	84	ND	ND	89
1c	C[b]	−1.13	1.9	ND	101	ND	ND	101

1 = starting material; **3** = phenylacetamide (**3a**, **3b**, **3c**); **4** = aniline (**4a**, **4b**); **5** = dimer (**5a**, **5b**).
[a] Yield expressed as the percentage of starting material incorporated into each species.
[b] For these experiments, 2.0 mM nickel(I) salen, electrogenerated at carbon (RVC), served as a catalyst.
[c] ND = species not detected.

peak gave *N*-phenylacetamide (**3c**) as the main product, along with unreduced starting material. Electrolyses of **1c** at potentials corresponding to the second cathodic peak at both cathodes afforded *N*-phenylacetamide (**3c**) as the only product, and very little (if any) of the starting material remained. Indirect (mediated) reduction of **1c** by electrogenerated nickel(I) salen led only to *N*-phenylacetamide (**3c**).

Because cyclic voltammograms for reduction of **1c** exhibit two cathodic peaks at both glassy carbon and silver electrodes (Fig. 1), we sought specific evidence for the generation of carbanionic intermediates at potentials corresponding to either or both of the cathodic peaks for reduction of this compound. Accordingly, controlled-potential (bulk) electrolyses of **1c** at both reticulated vitreous carbon and silver gauze cathodes were undertaken in the presence of both HFIP and D_2O. First, electrolyses of 5.0 mM solutions of **1c** in DMF–0.050 M $TMABF_4$ containing 50 mM HFIP were carried out at a potential corresponding to the first stage of reduction (E_{carbon} = −1.46 V and E_{silver} = −0.74 V). Reduction of **1c** afforded *N*-phenylacetamide (**3c**) as the only product in essentially quantitative yield (102–106%); coulometric *n* values were 2.7 for carbon and 2.2 for silver, and the unusually large *n* value obtained for carbon appears to be due to co-reduction of some HFIP. Second, bulk electrolyses of 5.0 mM solutions of **1c** in DMF–0.050 M $TMABF_4$ containing 50 mM D_2O were, once again, performed at both cathodes and at a potential corresponding to the first stage of reduction. For these experiments, the coulometric *n* values were 1.2 for carbon and 1.1 for silver; interestingly, and in accord with appropriate entries in Table 1, the product distribution consisted of unreduced starting material (**1c**) and *N*-phenylacetamide (**3c**), the latter being singly deuterated.

3.5. Conformations of 2-chloro-N-phenylacetamides (*1a*–*1c*)

Initial theoretical calculations were performed to identify the most stable conformations of the 2-chloro-*N*-phenylacetamides. We found that the lowest energy conformer (**CF1**) possesses a *trans* orientation, as shown in Fig. 4a; this conformer is approximately 6 kcal mol^{-1} more stable than the conformer (**CF2**) with a *cis* orientation (Fig. 4b). This finding is in agreement with previous conformational studies of amides [43–45]. With the more stable *trans* orientation as a starting point, mechanistic studies were carried out for the three derivatives (**1a**–**1c**) to understand our experimental findings. As discussed in the following sections, these calculations clearly reveal why the electrochemical behavior of **1a** and **1b** is different from that of **1c**.

3.6. Mechanistic features of the reduction of 2-chloro-N-methyl-N-phenylacetamide (*1a*) and 2-chloro-N-ethyl-N-phenylacetamide (*1b*) at glassy carbon and silver cathodes

On the basis of coulometric *n* values, product distributions, and theoretical calculations, a plausible set of pathways for the formation of each product is proposed in Scheme 1 for the reduction of **1a** and **1b** in DMF. Thus, 2-chloro-*N*-alkyl-*N*-phenylacetamide (**1a** or **1b**) initially undergoes one-electron reductive cleavage of the carbon–chlorine bond to give radical **2a** or **2b**, a step in accord with the coulometric *n* value of 1 (Table 1). Abstraction of a hydrogen atom from the solvent affords the major product (**3a** or **3b**). To explain the formation of the substituted aniline (**4a** or **4b**) during an electrolysis, we suggest that radical **2a** or **2b** eliminates ketene to yield a *N*-substituted aniline radical which abstracts a hydrogen atom from the solvent to form the observed product. Optimized structures for the radical species (**2a** and **2b**) as well as for the transition states for ketene elimination (**TS1a** and **TS1b**) are given in Fig. 5. Stretching of the N–C distance from 1.4 Å in **2** to 2.0 Å in **TS1** (for both the methyl and ethyl derivatives) clearly shows the process of bond breaking to form the ketene; the calculated Gibbs free energy of the transition states (**TS1a** and **TS1b**) for ketene elimination are very similar, 21 and 22 kcal mol^{-1}, respectively, with respect to the corresponding radical **2**. This finding is consistent with the observed experimental results where the amines (**4a** and **4b**) are formed as significant products via the electrochemical reduction of **1a** and **1b,** respectively. However, experimental attempts to verify directly the formation of the ketene by means

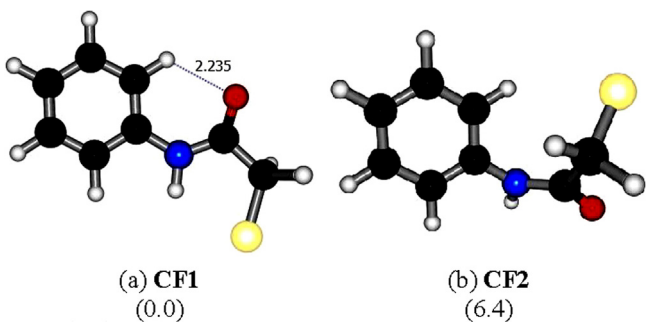

Fig. 4. Optimized geometries of lowest energy conformers (a) **CF1** and (b) **CF2** corresponding to the two different orientations, *trans* and *cis*, respectively. Given in parentheses for each conformer is the relative Gibbs free energy (kcal mol^{-1}) calculated at the B3LYP/6-31 + G(d,p) level.

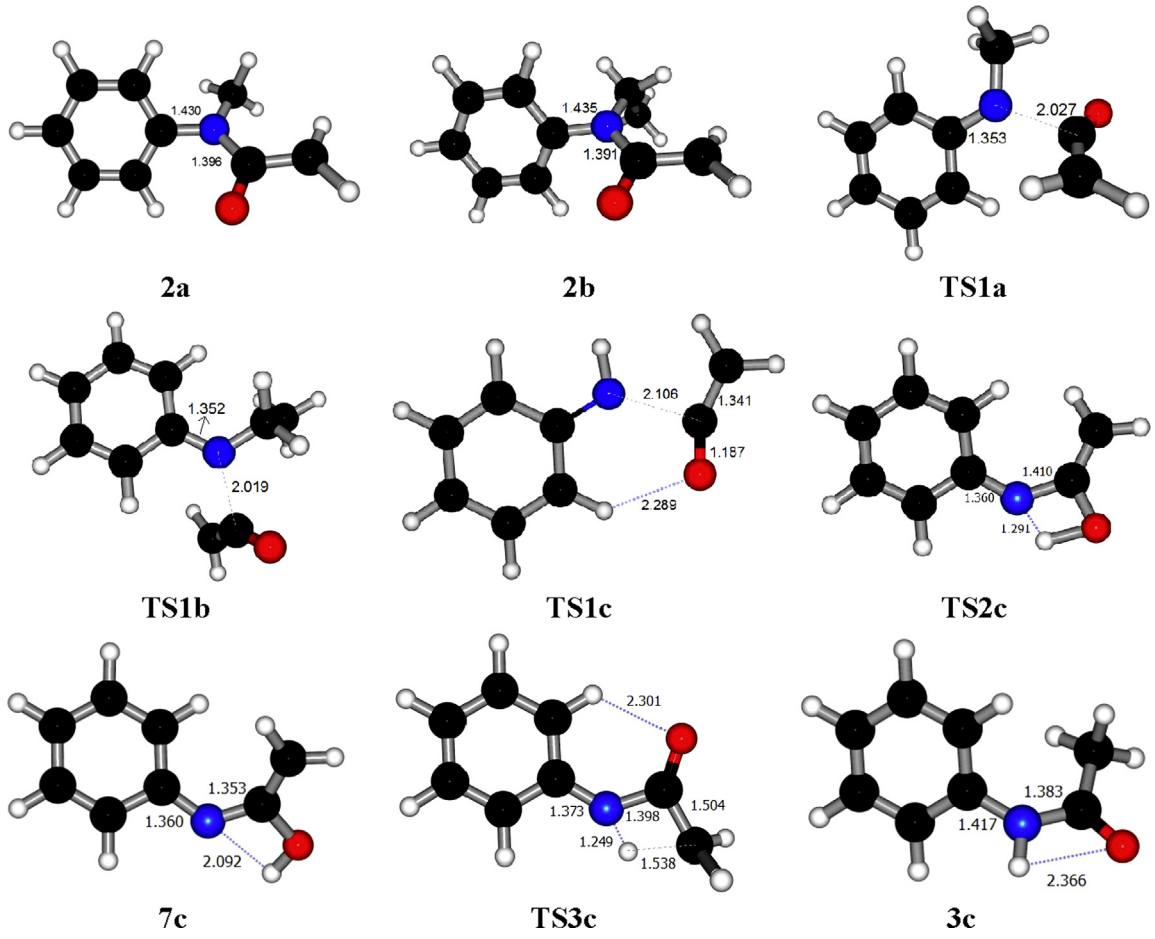

Fig. 5. Optimized geometries for reactive species (radicals and carbanions) generated by electrochemical reduction and for the transition states involved in various mechanistic steps.

of trapping with *tert*-butyl alcohol were unsuccessful [46]. Finally, formation of the dimer (**5a** or **5b**) as a minor product arises from combination of two radical species (**2a** or **2b**).

3.7. *Mechanistic features of the reduction of 2-chloro-N-phenylacetamide (**1c**) at glassy carbon and silver cathodes*

Theoretical calculations reveal that the electrochemical reduction of **1c** must take place via a mechanism different from what has just been described for the electrochemistry of **1a** and **1b**. Shown in Scheme 2 is our proposed set of mechanistic pathways for the reduction of **1c**. Experimentally, the coulometric measurements ($n \sim 2$) clearly suggest that **1c** undergoes a two-electron reduction to form a resonance-stabilized carbanion (**6c**) which, in the simplest mechanism, can extract a proton, most likely from residual water present in the solvent, to give the dehalogenated acetamide (**3c**). However, such a process does not explain why **1c** behaves very differently from **1a** and **1b**.

Our calculations suggest that proton migration in the carbanion is principally responsible for the differences seen in the behavior of **1c** in comparison with **1a** and **1b**. By first considering the involvement of a resonance form of carbanion **6c**, namely enolate **6c**′ in Scheme 2, we examined the migration of the proton from the N atom to the O atom via transition state **TS2c** (shown in Fig. 5 and Scheme 2), which leads to an anionic intermediate (**7c**). However, our calculations show that **7c** is less stable than **6c** by 10.9 kcal mol^{-1} (Table 2), so that **7c** is not likely to play a role in the reaction. This revelation led us to consider an alternative pathway wherein **6c** undergoes a proton migration from nitrogen to the carbanion site via **TS3c**, as depicted in Fig. 5 and Scheme 2. Interestingly, the resulting anion (**8c**), pictured in Scheme 2, is substantially more stable than carbanion **6c** by 14.8 kcal mol^{-1} (Table 2); therefore, the anion will readily convert from **6c** to **8c**. What follows is protonation of **8c** by the medium to form the observed product (*N*-phenylacetamide, **3c**). In addition, as shown at the bottom of Scheme 2, it is conceivable that **3c** could arise via proton transfer between **1c** and **6c**, leaving a (2-chloroacetyl)(phenyl)amide anion (**1c**$^{-}$) that is reducible to **3c** at potentials corresponding to the second cathodic peak seen in Fig. 1 for reduction of **1c**. A calculation, based on density functional theory, indicated that reductive cleavage of the carbon–chlorine bond of **1c** should be 0.38 V easier than that of **1c**$^{-}$. This result, which does not take into account any interaction between **1c**$^{-}$and the supporting–electrolyte cation (TMA^{+}), is consistent with the difference (0.54–0.55 V) in the cathodic peak potentials shown in Fig. 1 for the two-step reduction of **1c** at both glassy carbon and silver.

Table 2 compares the relative energies of the different stationary points for the one- and two-electron reduction of the three 2-chloro-*N*-phenylacetamides (**1a**–**1c**). Observed differences in the products arising from electrochemical reduction of these compounds can be attributed to the formation of the stable amide anion (**8c**). Because the migration of methyl and ethyl groups is unlikely, the amide anions (**8a** and **8b**) will not form. Without this additional stabilizing effect, reductions of **1a** and **1b** do not go through the anionic pathway, but follow the radical pathway considered earlier (Scheme 1). Moreover, even for **1c**, the formation of **8c** precludes elimination of ketene or dimerization reactions

Table 2
Relative energies of key stationary points involved in formation of the feasible products after one- and two-electron reduction of 2-chloro-*N*-phenylacetamides (**1a**–**1c**). Geometries were optimized at the B3LYP/6-31 + G(d,p) level of theory.

Coulometric *n* value	Starting compound	Stationary points	B3LYP/ 6-311 + +G(3df,2p)	$SMD_{(DMF)}$: B3LYP/ 6-311 + +G(3df,2p)
			ΔG	ΔG_{sol}
1	**1a**	**2a**	0.0	0.0
		TS1a	20.5	21.0
	1b	**2b**	0.0	0.0
		TS1b	20.9	21.9
	1c	**2c**	0.0	0.0
		TS1c	27.1	28.7
2	**1c**	**6c**	0.0	0.0
		TS2c	26.8	31.0
		7c	7.5	10.9
		TS3c	33.7	37.7
		8c	−17.0	−14.8

involving the anion. Thus, our calculations are in agreement with the observed experimental results for the electrochemical reduction of all three 2-chloro-*N*-phenylacetamides (**1a**–**1c**).

Finally, we considered the possibility of a radical pathway for reduction of **1c**. Experimental results for reduction of **1c** compiled in Table 1 do suggest that a radical pathway ($n = 1$) is operative, along with the anionic pathway ($n = 2$). Accordingly, reactions similar to those proposed for **1a** and **1b** are also conceivable for **1c**. To explore this point further, we obtained a transition state (**TS1c**, Fig. 5) for the elimination of ketene from **2c** (analogous to **2a** and **2b** in Scheme 1) that would lead to aniline as the product (not observed experimentally). As can be seen from Table 2, the free-energy barrier (~29 kcal mol^{-1}) of the transition state **TS1c** for ketene elimination from **2c**, that would be formed by one-electron reduction of **1c**, is significantly higher than the corresponding values for transition states **TS1a** and **TS1b** that arise, respectively, from reduction of **1a** and **1b**. This result suggests that ketene elimination from **2c** is not feasible at room temperature, unlike the situation for **2a** and **2b**. In addition, this conclusion is consistent with the observed experimental results where the alkyl-substituted aniline products (**4a** and **4b**) are formed via ketene elimination upon reduction of **1a** and **1b**, respectively. In the case of **2c**, hydrogen atom abstraction from the solvent then leads to the observed product (**3c**).

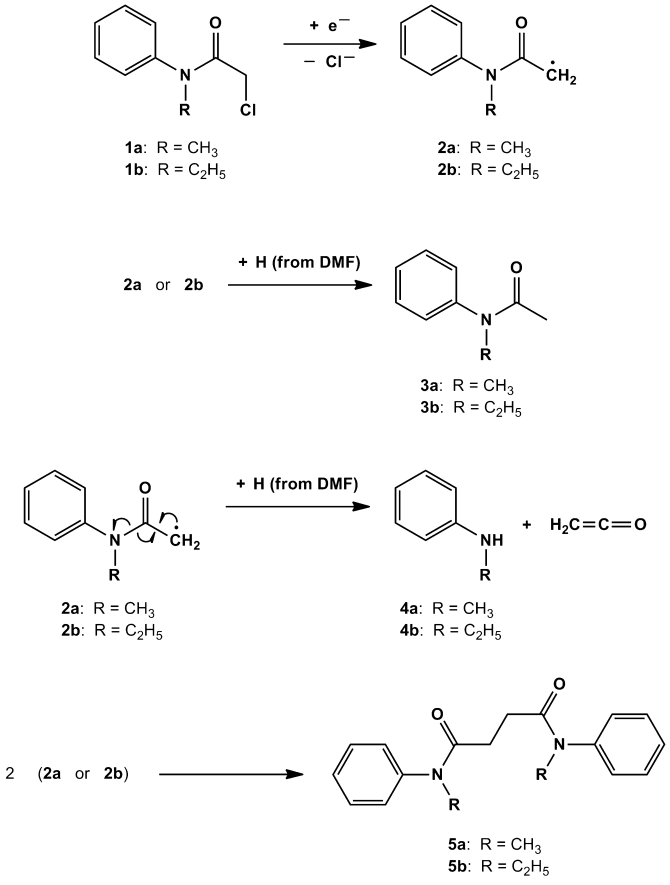

Scheme 1. Proposed mechanistic scheme for electrochemical reductions of **1a** and **1b** at reticulated vitreous carbon and silver gauze cathodes in DMF–0.050 M $TMABF_4$.

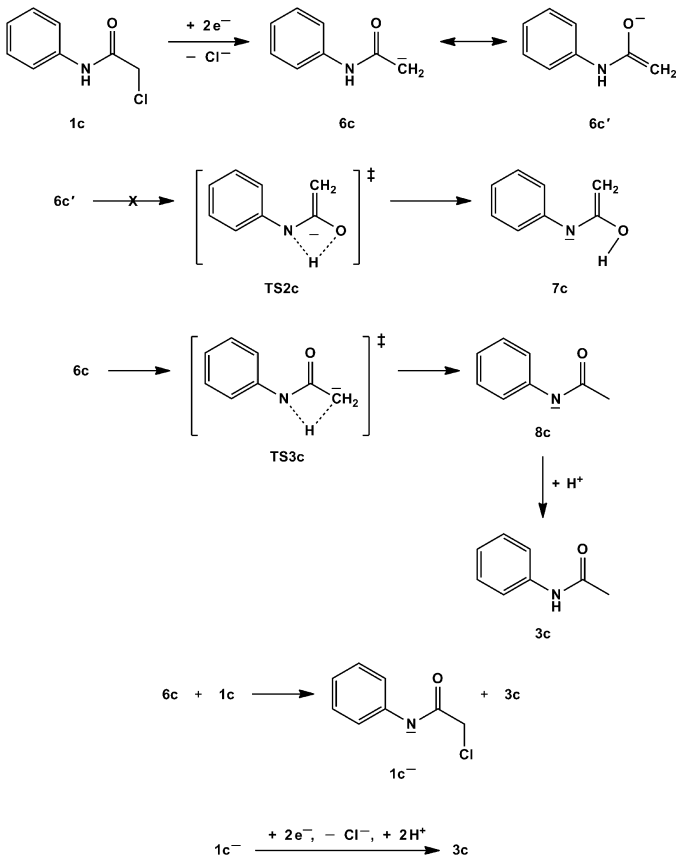

Scheme 2. Proposed mechanistic scheme for electrochemical reduction of **1c** at reticulated vitreous carbon and silver gauze cathodes in DMF–0.050 M $TMABF_4$.

Acknowledgments

This work was supported in part by Department of Energy Grant No. DE-FG02-07ER15889 to K. R.

Appendix A. Supplementary data

Supplementary data associated with this article can be found, in the online version, at http://dx.doi.org/10.1016/j.electacta.2014.01.133.

References

[1] I. Carelli, A. Inesi, M.A. Casadei, B. Di Rienzo, F.M. Moracci, Electrochemical behaviour of halogenoamides. The role of additional functional groups on the reduction pattern and the nature of the products, Journal of the Chemical Society, Perkin Transactions 2 (1985) 179.
[2] F. Maran, E. Vianello, G. Cavicchioni, F. D'Angeli, Electrochemical reduction of 2-bromo-carboxamides. Self-protonation mechanism and reaction with dimethylformamide, Journal of the Chemical Society, Chemical Communications (1985) 660.
[3] I. Carelli, A. Inesi, V. Carelli, M.A. Casadei, F. Liberatore, F.M. Moracci, Electrochemical studies of β-lactams; Part 2. Electrosynthesis of β-lactams via bond formation between C-3 and C-4, Synthesis (1986) 591.
[4] F. Maran, E. Vianello, F. D'Angeli, G. Cavicchioni, G. Vecchiati, Electrochemistry of 2-bromo-2-methylpropanamides. Reduction mechanism and cyclocoupling reaction with amide solvents, Journal of the Chemical Society, Perkin Transactions 2 (1987) 33.
[5] F. Maran, M. Fabrizio, F. D'Angeli, E. Vianello, Electro-carboxylation of 2-bromoisobutyramides. A useful synthetic way to ester-amides of 2,2-dimethylmalonic acid, Tetrahedron 44 (1988) 2351.
[6] M.A. Casadei, A. Gessner, A. Inesi, W. Jugelt, H. Liebezeit, F.M. Moracci, 2. Electrochemical behavior of ω-bromoalkanamides. Electrosynthesis of β-, γ-, and δ-lactams, Bulletin de la Société Chimique de France (1989) 650.
[7] F. Maran, S. Roffia, M.G. Severin, E. Vianello, Study on a proton transfer reaction between electrogenerated carbon bases and parent nitrogen acids, Electrochimica Acta 35 (1990) 81.
[8] M.A. Casadei, B. Di Rienzo, A. Inesi, F.M. Moracci, Electrochemical studies on haloamides. Part 3. Haloacetamides and haloacetohydroxamates, Journal of the Chemical Society, Perkin Transactions 1 (1992) 375.
[9] F. Maran, Electrochemical and stereochemical investigation on the mechanism of the decay of 2-halo amide anions. The intermediacy of aziridinones, Journal of the American Chemical Society 115 (1993) 6557.
[10] M.A. Casadei, S. Cesa, A. Inesi, Electrochemical studies on haloamides. Part XII. Electrosynthesis of oxazolidine-2,4-diones, Tetrahedron 51 (1995) 5891.
[11] M.A. Casadei, S. Cesa, A. Inesi, F. Micheletti, Electrochemical studies on haloamides. Part 11. Electrocarboxylation of carboxamides, Journal of Chemical Research (1995) 166.
[12] M. Feroci, M. Orsini, L. Palombi, L. Rossi, A. Inesi, An electrochemical alternative strategy to the synthesis of β-lactams via N–C4 bond formation, Electrochimica Acta 50 (2005) 2029.
[13] M. Feroci, M. Orsini, L. Rossi, G. Sotgiu, A. Inesi, An electrochemical alternative strategy to the synthesis of β-lactams. Part 2. C3-C4 bond formation, Electrochimica Acta 51 (2006) 5540.
[14] G. Sotgiu, I. Chiarotto, M. Feroci, M. Orsini, L. Rossi, A. Inesi, An electrochemical alternative strategy to the synthesis of β-lactams. Part 3. Room-temperature ionic liquids vs molecular organic solvents, Electrochimica Acta 53 (2008) 7852.
[15] E.J. Hennessy, S.L. Buchwald, Synthesis of substituted oxindoles from α-chloroacetanilides via palladium-catalyzed C–H functionalization, Journal of the American Chemical Society 125 (2003) 12084.
[16] J. Kopilov, D.H. Evans, Electrochemical reduction of some α-haloacetanilides, Journal of Electroanalytical Chemistry 280 (1990) 435.
[17] K.L. Vieira, D.G. Peters, Voltammetric behavior of tertiary butyl bromide at mercury electrodes in dimethylformamide, Journal of Electroanalytical Chemistry 196 (1985) 93.
[18] L.W. Marple, Reference electrode for anhydrous dimethylformamide, Analytical Chemistry 39 (1967) 844.
[19] C.W. Manning, W.C. Purdy, Reference electrode for electrochemical studies in dimethylformamide, Analytica Chimica Acta 51 (1970) 124.
[20] J.L. Hall, P.W. Jennings, Modification of the preparation of a cadmium amalgam reference electrode for use in N,N-dimethylformamide, Analytical Chemistry 48 (1976) 2026.
[21] L.M. Strawsine, M.S. Mubarak, D.G. Peters, Use of silver cathodes to promote the direct reduction and intramolecular cyclization of ω-halo-1-phenyl-1-alkynes in dimethylformamide, Journal of The Electrochemical Society 160 (2013) G3030.
[22] P. Vanalabhpatana, D.G. Peters, Catalytic reduction of 1,6-dihalohexanes by nickel(I) salen electrogenerated at glassy carbon cathodes in dimethylformamide, Journal of The Electrochemical Society 152 (2005) E222.
[23] J.A. Cleary, M.S. Mubarak, K.L. Vieira, M.R. Anderson, D.G. Peters, Electrochemical reduction of alkyl halides at vitreous carbon cathodes in dimethylformamide, Journal of Electroanalytical Chemistry 198 (1986) 107.
[24] W.A. Pritts, K.L. Vieira, D.G. Peters, Quantitative determination of volatile products formed in electrolyses of organic compounds, Analytical Chemistry 65 (1993) 2145.
[25] M.J. Frisch, G.W. Trucks, H.B. Schlegel. G.E. Scuseria, M.A. Robb, J.R. Cheeseman, G. Scalemani, V. Barone, B. Mennucci, G.A. Pettersson, et al., Gaussian 09, revision h08; Gaussian, Inc.; Wallington, CT, 2009.
[26] A.D. Becke, Density-functional thermochemistry. III. The role of exact exchange, Journal of Chemical Physics 98 (1993) 5648.
[27] C. Lee, W. Yang, R.G. Parr, Development of the Colle-Salvetti correlation-energy formula into a functional of the electron density, Physical Review B 37 (1988) 785.
[28] P.C. Hariharan, J.A. Pople, Influence of polarization functions on MO hydrogenation energies, Theoretica Chimica Acta 28 (1973) 213.
[29] M.M. Francl, W.J. Pietro, W.J. Hehre, J.S. Binkley, M.S. Gordon, D.J. DeFrees, J.A. Pople, Self-consistent molecular orbital methods. XXIII. A polarization-type basis set for second-row elements, Journal of Chemical Physics 77 (1982) 3654.
[30] R. Krishnan, J.S. Binkley, R. Seeger, J.A. Pople, Self-consistent molecular orbital methods. XX. A basis set for correlated wave functions, Journal of Chemical Physics 72 (1980) 650.
[31] J.-P. Blaudeau, M.P. McGrath, L.A. Curtiss, L. Radom, Extension of Gaussian-2 (G2) theory to molecules containing third-row atoms K and Ca, Journal of Chemical Physics 107 (1997) 5016.
[32] A.V. Marenich, C.J. Cramer, D.G. Truhlar, Universal solvation model based on solute electron density and on a continuum model of the solvent defined by the bulk dielectric constant and atomic surface tensions, Journal of Physical Chemistry B 113 (2009) 6378.
[33] C. Gonzalez, H.B. Schlegel, Reaction path following in mass-weighted internal coordinates, Journal of Physical Chemistry 94 (1990) 5523.
[34] C. Gonzalez, H.B. Schlegel, An improved algorithm for reaction path following, Journal of Chemical Physics 90 (1989) 2154.
[35] A.A. Peverly, J.A. Karty, D.G. Peters, Electrochemical reduction of (1R,2r, 3S,4R,5r,6S)-hexachlorocyclohexane (Lindane) at silver cathodes in organic and aqueous–organic media, Journal of Electroanalytical Chemistry 692 (2013) 66.
[36] E.R. Wagoner, D.G. Peters, Electrocatalytic reduction of 1,1,2-trichloro-1,2,2-trifluoroethane (CFC-113) at silver cathodes in organic and organic–aqueous solvents, Journal of The Electrochemical Society 160 (2013) G135.
[37] A.A. Peverly, E.M. Pasciak, L.M. Strawsine, E.R. Wagoner, D.G. Peters, Electrochemical reduction of decabromodiphenyl ether at carbon and silver cathodes in dimethylformamide and dimethyl sulfoxide, Journal of Electroanalytical Chemistry 704 (2013) 227.
[38] S. Rondinini, A. Vertova, Electrocatalysis on silver and silver alloys for dichloromethane and trichloromethane dehalogenation, Electrochimica Acta 49 (2004) 4035.
[39] A.A. Isse, G. Sandonà, C. Durante, A. Gennaro, Voltammetric investigation of the dissociative electron transfer to polychloromethanes at catalytic and non-catalytic electrodes, Electrochimica Acta 54 (2009) 3235.
[40] O. Scialdone, C. Guarisco, A. Galia, R. Herbois, Electroreduction of aliphatic chlorides at silver cathodes in water, Journal of Electroanalytical Chemistry 641 (2010) 14.
[41] M.A. Ischay, M.S. Mubarak, D.G. Peters, Catalytic reduction and intramolecular cyclization of haloalkynes in the presence of nickel(I) salen electrogenerated at carbon cathodes in dimethylformamide, Journal of Organic Chemistry 71 (2006) 623.
[42] D.M. Goken, M.A. Ischay, D.G. Peters, J.W. Tomaszewski, J.A. Karty, J.P. Reilly, M.S. Mubarak, Alkyl group incorporation into nickel salen during controlled-potential electrolyses in the presence of alkyl halides, Journal of The Electrochemical Society 153 (2006) E71.
[43] L.A. LaPlanche, M.T. Rogers, Cis and trans configurations of the peptide bond in N-monosubstituted amides by nuclear magnetic resonance, Journal of the American Chemical Society 86 (1964) 337.
[44] F.A. Bovey, J.J. Ryan, F.P. Hood, Polymer nuclear magnetic resonance spectroscopy. XV. The conformation of polysarcosine, Macromolecules 1 (1968) 305.
[45] A.E. Tonelli, Stability of cis and trans amide bond conformations in polypeptides, Journal of the American Chemical Society 93 (1971) 7153.
[46] C.A. Snyder, J.P. Selegue, E. Dosunmu, N.C. Tice, S. Parkin, C,O-dialkylation of Meldrum's acid: Synthesis and reactivity of 1,3,7,7-tetramethyl-4H,10H-6,8,9-trioxa-2-thiabenz[f]azulen-5-one, Journal of Organic Chemistry 68 (2003) 7455.